Supplementary Information

A low-cost biocompatible and biodegradable multipurpose resistive ink for monitoring biological systems

Akshayakumar Kompa, Revathi Ravindran, Jianyu Hao, Javier G Fernandez*

* jgomez@ibecbarcelona.eu (JGF)

This material includes:

Materials and Methods

Informed consent for experiments involving humans: Informed consent was obtained from all individual participants included in the study. Participants were provided with detailed information about the study's purpose, procedures, and potential risks. They were given the opportunity to ask questions and voluntarily agreed to participate without any coercion.

Materials: Chitosan was sourced from the residual materials of shrimp processing factories in India, courtesy of iChess Pvt. Ltd., Mumbai, India. Industrial-grade acetic acid and Carbon Black (Tedpilla, particle size is 30 nm) were obtained from local vendors and utilized as received.

Ink/sample preparation: For ink preparation, a 3% chitosan solution was prepared by dissolving chitosan powder in 1% acetic acid with continuous stirring for 48 hours at standard temperature to ensure a homogeneous solution. 1.9% v:v glycerol was added to this solution, followed by carbon black (1.9%, 3.7%, and 5.5% w:v). The mixture was ultrasonicated for 10 min and stirred for 24 hours. For the physical and chemical characterization of the ink, standard samples were prepared by depositing and drying a few drops of ink on a petri dish at standard temperature and pressure.

Crystalographic characterization: The crystallographic structure of the polymers was identified using an X-ray diffractometer (Empyrean, Malvern Panalytical Ltd., UK) attested with Cu as anode material to generate CuKα radiation. The patterns were recorded at room temperature using a continuous scan type between 5° and 50° with a step size of 0.008°.

Surface morphology imaging: The morphology of the samples was characterized using Scanning electron microscopy (JEOL-JSM-7600F). Before imaging, samples were gold-coated to render the surface conductive.

FTIR study: Fourier transform Infrared (FTIR) information was recorded using a spectrometer (VERTEX 70 FT-IR, Bruker, USA) in attenuation total reflection (ATR) in the range between 4000-400 cm^{-1} with a resolution of 4 cm^{-1}.

XPS study: The orbital level information was obtained using an x-ray photoelectron spectroscope (AXIS Supra+, Kratos Analytical, UK). It was operated using AlKα as the X-ray source, a wide scan with a pass energy of 160 eV (1 eV step size), and a narrow scan with a 20 eV (0.1 eV step size). The data obtained was analyzed using CasaXPS (Casa Software Ltd.). The standard carbon C1s peak (284.8 eV) was used as the reference for calibration, and the Shirley method was used for background correction. The data was deconvoluted using Gaussian Lorentzian (GL-30) line shape function to determine the films' oxidation state and elemental composition.

TGA measurement: The loss of water content and decomposition temperatures were studied using thermogravimetric analysis (Q50, TA Instruments, USA). The samples were heated between 30 to 600 °C with a ramp rate of 10 °C/min in a nitrogen atmosphere.

Sensor measurements: The relative resistance changes of the strain sensors were tested using a benchtop digital multimeter (Multicomp Pro MP730027, Premier Farnell Ltd., UK). The relative change in resistance was computed as:

$$\Delta R\ (\%) = \left(\frac{R - R_o}{R_o}\right) \times 100$$

Where ΔR is the relative change in resistance, R_0 is the initial resistance before applying strain, and R is the resistance after applying strain. The sensitivity or gauge factor (GF) was calculated as:

$$GF = \frac{\Delta R}{\varepsilon}$$

Where ε is the applied strain.

Heart pulsation measurement: Pig (*sus domesticus*) hearts were acquired from local vendors and used as received. To replicate the native movement of the heart, we utilized a custom-built pneumatic system. This system consisted of a 50 ml syringe that pumped water through a 1 cm diameter PTFE tube into the heart's atrium. The experimental sensor element was directly painted onto the heart and allowed to dry for ten minutes. Two copper wires with a diameter of 0.202 mm (32 AWG) were placed on the heart's surface, where the ends of the painted electrode were later located. The ends of these wires were subsequently covered with the ink when the sensor was painted. Once the ink dried, the wires were effectively integrated with it, enabling their connection to a multimeter for measuring the resistance across the paint.

Digitalization of hand movements: The armature feature in Blender (Blender Online Community) was used to create the bones for the animation. Each finger was given the same number of bones corresponding to an actual finger. Spheres between each bone, acting as the rotational pivot points essential for bending movements, were used as digital replacements for the joints. Once the bone wireframe was set up, the influence of each bone on each vertex of the hand model was automatically calculated, enabling a correlation between the virtual bones' and virtual hand's movements. Once the structure and constraints of the hand were established, the bones were animated using four basic movements: i) Hand extended and held, ii) closing into a fist, iii) fist hold, and iv) Fist opening. The timing of the movement was matched with the changes in resistance corresponding to each of the transitions between positions as recorded by the multimeter using a real hand.

Soil burial test. The biodegradability of the samples was evaluated using a soil burial test. Standalone dry ink samples measuring approximately 20 mm × 20 mm were weighted and buried in the compost mixture at a depth of 8 cm. Due to the rapid degradation of the samples in the standard compost composition, a dried version of the standard composting soil, which consisted of equal parts organic compost, organic material, and topsoil, was used.

Tensile test. The mechanical properties of the dried ink were assessed through a standard tensile test (ISO 527-3). Freestanding films were prepared by placing several drops of the ink into Petri dishes and drying them in an oven at 40 °C to remove water content. The dried films were then carefully extracted and cut into appropriate sizes for testing. Tensile strength

measurements were performed at ambient room temperature using a 5980 Series Universal Testing Machine (Instron, MA, US).

Tables

Ink type	Cost (USD)	Sensitivity	Versatility	Environmental impact	Manufacturer
Silver ink	$257.80 for 10gm	5-6 μΩ cm	Flexible and circuit electronic applications	Very toxic to aquatic life with long lasting effects	Sigma-Aldrich
Graphene	$51.12/25ml	12 Ω/sq	Flexible and flexography electronics, wearable electronics, thermal applications	Moderate due to volatile solvents, long-term degradation products may develop over time	Techinstro
Silver	$183.80/5ml	0.10 Ω/sq	For screen printing applications	Very toxic to aquatic life with long lasting effects	Sigma-Aldrich
MWCNT	$107.44/25ml	7.2 Ω for line thickness: 0.04mm	Screen printing and flexible electronics	Water-based ink with low impact on the environment.	Techinstro
Graphene/ PEDOT: PSS	$420.78/50 ml	500 Ω/sq	Printing technology, solar cells, and capacitors	PEDOT: PSS is not biodegradable	Sigma-Aldrich
Carbon ink	$10.37/30 gm	130 Ω/sq	Flexible electronics	Hazardous decomposition may involve oxides of carbon, toxic fumes, and gases emitted upon decomposition.	Tedpella
Chitosan-Carbon ink	$38/1L	105 Ω/sq	Flexible and wearable electronics	No harmful effect on the environment, easily degradable in a short period.	Current work

Table S1. Comparative analysis of conductive inks: Comparison of the cost, sensitivity, versatility, and environmental impact of Chitosan-Carbon ink with existing inks.

Figures

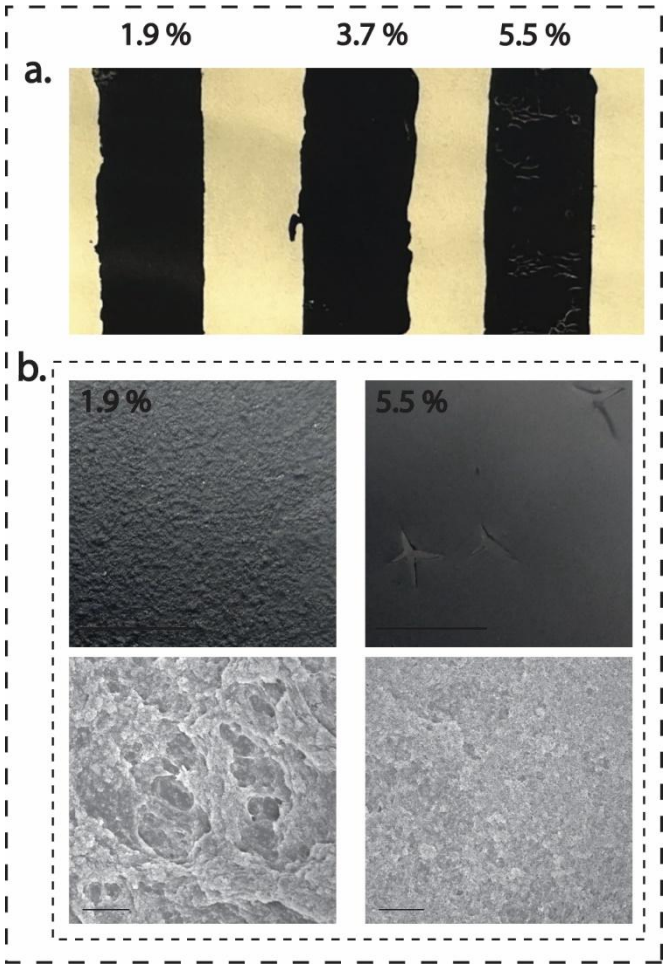

Figure S1. Optical and electron microscope images of samples: a. The Doctor blade method was used to coat ink samples onto a paper substrate, followed by drying in a hot air oven at 50°C. At 5.5% loading, the sample displayed surface cracks due to the brittleness induced by high concentrations of carbon content, and **b.** Optical images (scale bar: 1.5 cm) of free-standing film samples at 1.9% and 5.5% loading reveal distinct features. At 1.9% loading, visible lumps of carbon content are apparent. Meanwhile, at 5.5% loading, although the distribution appears uniform, the sample exhibits brittleness with noticeable macro cracks. Electron microscopy images (scale bar: 1 µm) of the same samples highlight clear differences in carbon distribution. Importantly, no visible agglomeration is observed under the electron microscope, confirming uniform distribution despite the brittleness observed at higher loading concentrations.

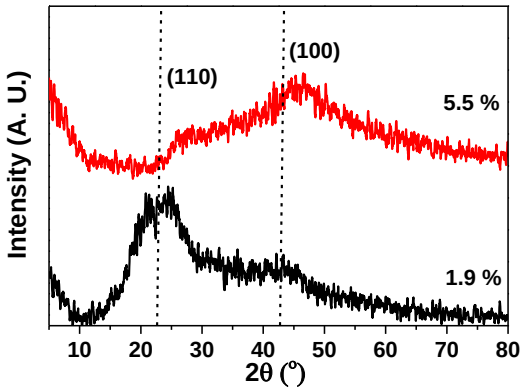

Figure S2. XRD pattern for Cs with 1.9% and 5.5% loading: The sample loaded with 1.9% CB remains amorphous yet retains a structure closely resembling pure CS [1]. However, at a higher loading of 5.5% CB, significant deformation occurs, with CB peaks dominating over CS. This indicates that the host structure is compromised by the excessive CB content. The sample with 5.5% CB loading is notably more brittle due to the excess CB, which suggests that cracks may occur upon application, such as painting. Therefore, achieving an optimal CB loading is essential to balance structural integrity and material properties.

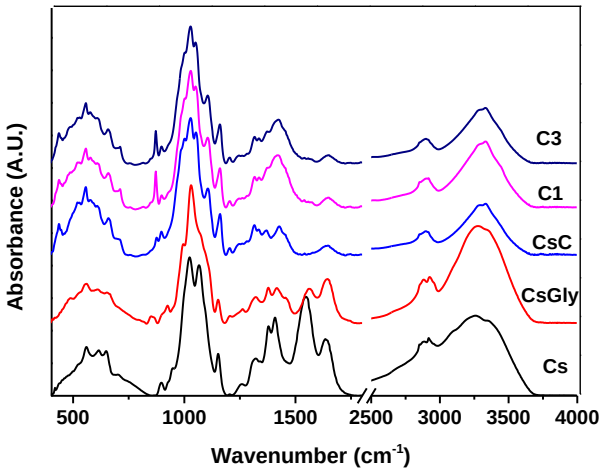

Figure S3. FTIR spectra of Cs, Cs-glycerol, Cs-C, Cs with 1.9% and 5.5% loading: Even though sample with 1.9% Cb loading is amorphous but retain its structure close to pure CS [2]. but high loading (5.5%) resulted in high deformation with CB peaks dominating over Cs. An optimized doping is necessary to retain the host structure, but exceeding solubility may result in complete distortion. The latter sample is more brittle due to excess CB thus we thus we can expect cracks when painted.

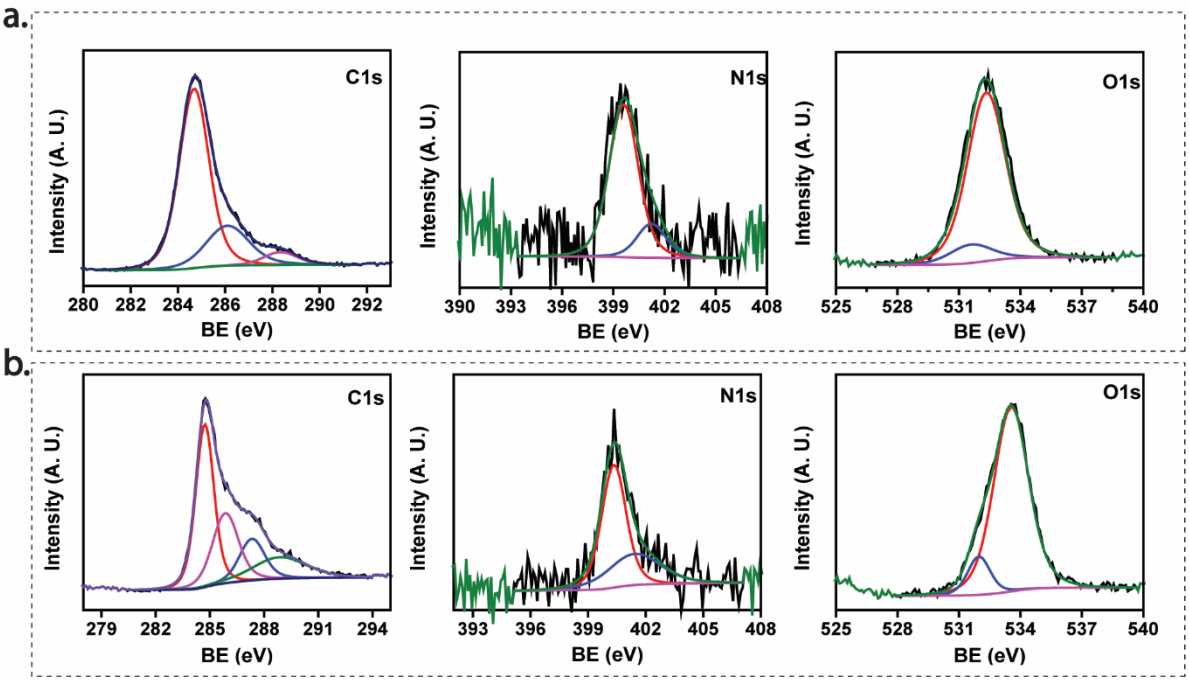

Figure S4. XPS narrow scans of C1s O1s, and N1s for 1.9% and 5.5% loaded samples: a. The high-resolution spectrum of carbon (C1s), nitrogen (N1s), and oxygen (O1s) for the 1.9% loaded sample reveals distinct bonding characteristics. In the C1s spectrum, the three peaks confirm the presence of C-C, C-O/C-N, and N-C-O bonding types. The N1s spectrum confirms the presence of amide and C-N bonding, while the deconvoluted peaks in the O1s spectrum confirm C=O and O-C bonding, and **b.** For the 5.5% loaded sample, the high-resolution spectrum shows an additional peak of C=O that was masked in the previous spectrum due to high hydroxyl group linkage to the carbon surface. This additional peak is visible in both the nitrogen and oxygen spectra. Additionally, the nitrogen spectrum and oxygen spectrum confirm respective peaks corresponding to amide, C-N, C=O, and O-C bonding. The strong, sharp peak at 284.8 eV in the C1s spectrum indicates uniform linkage of C-C throughout the sample. The presence of additional peaks for C-N/C-O and N-C-O further confirms interactions with chitosan and glycerol.

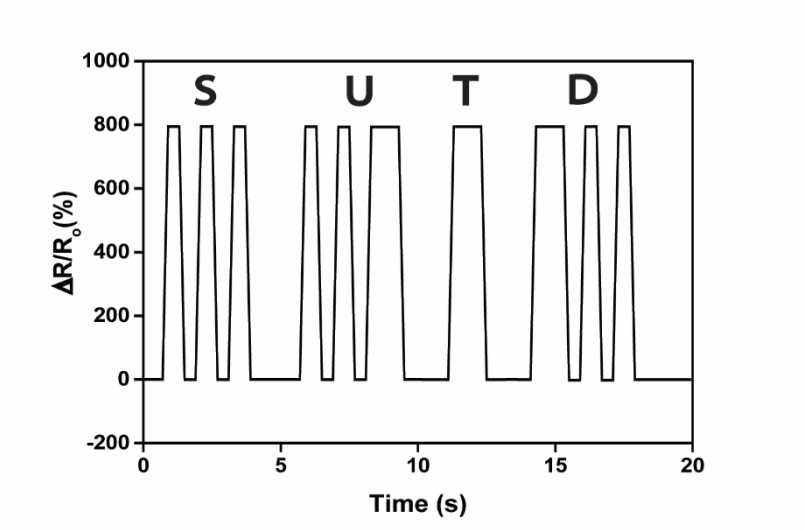

Figure S5. Transmitting morse code for SUTD by bending the finger: The plot illustrates the relative change in resistance, represented by dotted and dashed lines, during both short-term and long-term bending of the finger. This unique method enables the identification of communication through the sensor.

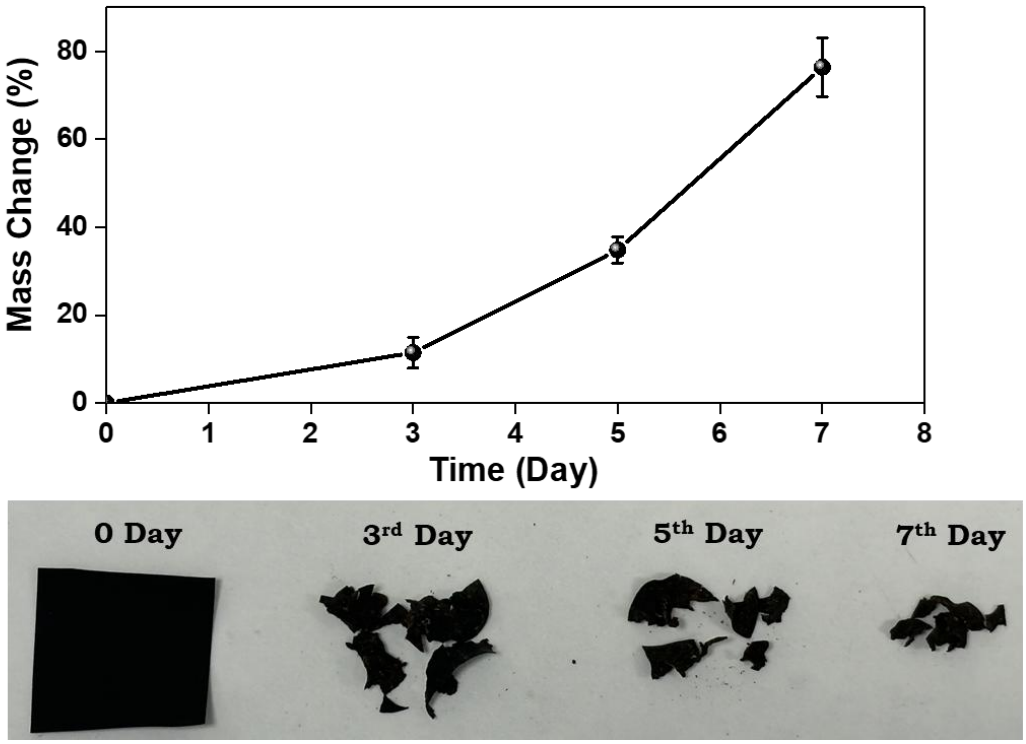

Figure S6. Biodegradation study: Soil burial test assessing the degradation of the sensor material (dried ink) over a period of 7 days. The results, illustrated by the plot and images, indicate very fast degradation in the soil. By the 7th day, the samples were found in small pieces distributed throughout the soil, with an average half-life of 6 days. It is worth noting that, due to the ink's solubility, the test had to be conducted in unusually dry soil rather than the standard 60% moisture because the ink degrades within hours under standard conditions.

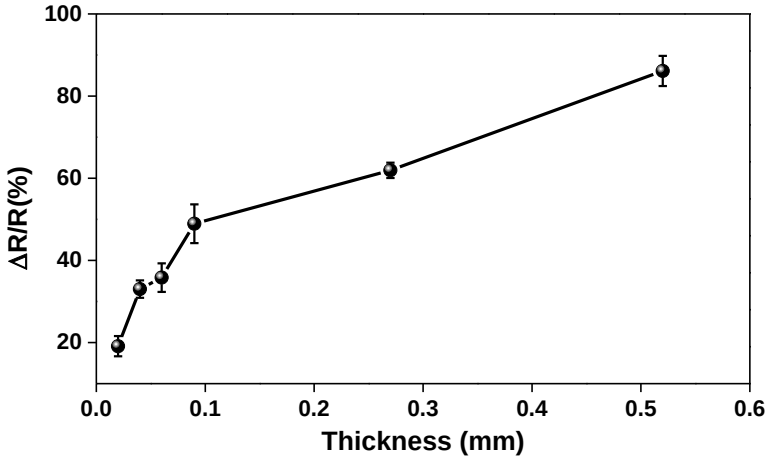

Figure S7. Thickness-dependent resistance variation: Relative change in resistance during controlled bending as a function of film thickness. As film thickness increases, the formation of cracks becomes more pronounced, leading to a significant variation in resistance values. Thinner sensors consistently offer greater flexibility without compromising performance, while thicker films become stiffer, making them less suitable for flexible electronics.

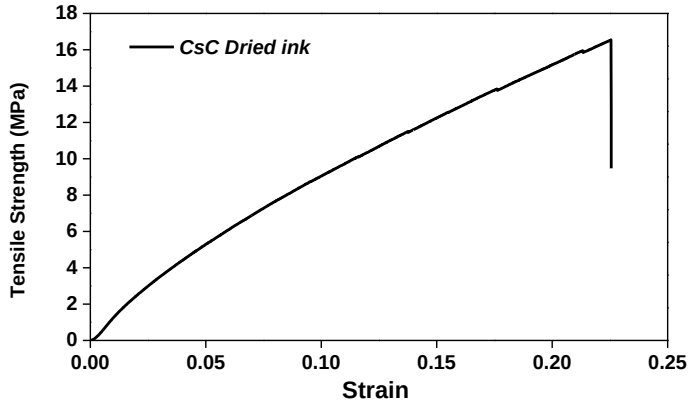

Figure S8. Mechanical strength of dried ink: The Cs solution loaded with CB was dried and subjected to mechanical testing using a 5980 Series Universal Testing Machine to determine its tensile strength. The film exhibited a tensile strength of 13.51 MPa at ambient room temperature. Whereas previous work [3] on chitosan filled with carbon nanotube has showed high tensile strength (~50 MPa) but flexibility has reduced with loading compared to current work.

Videos

Sup. Video 1 – Hand movement recording test. Video showcasing examples of hand movements recorded using customized resistive drawings made with plasticized chitosan/carbon black ink. A piece of copper tape is placed at each end of the drawing and connected directly to a multimeter, which records the changes in electrical resistance across the drawing.

Sup. Video 2 – Recording larynx vibrations (voice). The video shows the electrical resistance change across a line painted on the neck with plasticized chitosan/carbon black ink. Both ends of the painting are connected to a multimeter using thin copper wires. A clear and consistent change in electrical resistance can be observed every time the subject says "Hey".

Sup. Video 3 – Recording hand movements and use to produce a digital twin. A line painted on the knuckles of a test subject using plasticized chitosan/carbon black paint is used to monitor the state of the hand by measuring the electrical resistance across it. The resistance is measured by placing two copper wires at both ends and connecting them to a multimeter. The electrical resistance varies by three orders of magnitude, from a few kΩ to MΩ, depending on the state of the hand. This variation in resistance is used to update the state of a virtual hand representation.

Sup. Video 4 – Recording simulated beating of a heart. A line painted on the surface of a pig (*Sus domesticus*) heart with plasticized chitosan/carbon black ink is used to monitor its artificial beating. Two copper wires are connected to the ends of the line and to a multimeter to measure changes in electrical resistance. A PTFE tube is connected to the heart's atrium through the vein and stitched in place. An external pneumatic pump forcing DI water in and out of the cavity at regular intervals was used to simulate the usual movement of a beating heart.

Sup. Video 5 – Uses of the ink with medical bandages. Demonstration of the ink's application in modifying a standard plaster, transforming it into a "smart" plaster with the capability to measure movement. The video also showcases the direct application of the ink onto the skin in combination with standard wound protection, illustrating its performance when integrated with other medical devices and the ink's functionality under water conditions.

References

[1] K.J.T. Balasubramanian Rukmanikrishnan, Javier G. Fernandez, Secondary Reorientation and Hygroscopic Forces in Chitinous Biopolymers and Their Use for Passive and Biochemical Actuation, Advanced Materials Technologies, 8 (2023) 2300639.
[2] H.Z. Yongwang Liu, Mingxian Liu, High performance strain sensors based on chitosan/carbon black composite sponges, Materials & Design, 141 (2018) 276-285.
[3] L.S. Shao-Feng Wang, Wei-De Zhang and Yue-Jin Tong, Preparation and Mechanical Properties of Chitosan/Carbon Nanotubes Composites, Biomacromolecules, 6 (2005) 3067-3072.